Bioderived PolyHIPE Hydrogels Designed for Improving Water Scarcity Solutions

Ryan Zowada & Reza Foudazi

New Mexico State University

1. Introduction

Water retention in soil for arid climates is a main concern for agriculture, the largest consumer of fresh water. [1–3] These regions typically have high water loss due to both climate issues (low humidity and high temperature) and soil issues (high drainage loss due to sand). While there are solutions that act as immediate solutions such as SAPs (petroleum based synthetic polymers), they are non-biodegradable and have the potential to lose functionality. [4–6] Since SAPs are considered non-degradable, they are also excluded from emerging markets such as "organic farming," that require soil additives to have degradation pathways. There are other fields that would also greatly benefit from bio-based hydrogel foams such as bioengineering for cell viability and biocompatibility, and industries such as packaging or personal care product manufacturing that are searching for more sustainable options for foam material in their products. Specifically for agricultural purposes these biodegradable hydrogel foams can act as a water reservoir for plants between irrigation cycles to reduce water stress. Due to the capillary action from their porous nature the foams can both reduce water loss through gravimetric drainage and also increase water availability by holding water in the voids rather than the polymer network.

Biobased material's water sorption capabilities pale in comparison to SAPs due to the fundamental difference in their molecular structures. There have been methods to reach this high swelling capacity; however, these works typically rely on grafting synthetic polymers like polyacrylate (common in SAPs) onto the biopolymer or require a double polymer network system with similar synthetic polymers. [7–12] So, the water sorption capabilities still rely on the use of synthetic polymers. Further work is required where the biopolymer is the main material. Increasing porosity of biopolymer hydrogels can significantly increase the water holding potential due to capillary action. There has been previous research involving the use of bio-based polymers as a base material for hydrogel foams.[13,14] One common method for fabricating these foams is through energy intensive lyophilization (freeze-drying) or gas-generating reactions that produces a non-controllable morphology. These applications have potential at small application ratees (such as biomedical purposes), but for large application rates (agriculture or landscaping) there needs to be a scalable cost-effective approach for these materials. Emulsion-templating is a potential method in creating porous materials especially with high internal phase emulsion (HIPE) templates. HIPEs are emulsions where the disperse droplet phase surpasses 74 vol.% of the total emulsion and the droplets begin to deform from spheres into polyhedral shapes. [15–17] The thinning of the walls between droplets propagates interconnectivity of the resulting voids due to the thinning during drying, and this interconnectivity of the porous material results in high capillary action. While these systems are more stable than foams, these methods typically result in low starting material efficiency since >74% of the total volume is a sacrificial template and can also become a costly fabrication method for large-scale applications (agriculture). One method in which a templating approach can be more economical is by using a cheaper template material.

Biopolymer based foam templates can potentially be a solution to many issues including water scarcity by using a foaming mechanism that can reliably produce an interconnected porous foam. Unlike emulsion templates foam templates are unstable systems due to rapid coalescence of bubbles. Due to this instability, there is a requirement for a rapid crosslinking mechanism in order to achieve porous solid foams. Previous work that utilized grafted synthetic polymers on biopolymers could potentially be used for these systems because they still rely on rapid free radical polymerization for crosslinking, [7–12,18–21] this polymerization method is backed by previous work. [22] One possible mechanism that could be utilized for foam-templated systems are biopolymer networks that can be ionically crosslinked (,e.g., alginate,[18–21] Xanthan gum[23] and guar gum[24]). The porous network could be instantaneously immobilized and then covalently crosslinked in a 2-step crosslinking method.

The focus on this work is a one-step covalent crosslinking between chitosan and glutaraldehyde. Previous work indicates glutaraldehyde is a rapid crosslinking agent for amine functional groups under acidic conditions. [25–27] This makes chitosan ideal due to its requirement for a low pH water-acid solution in order to be dissolved. There are other benefits to the use of chitosan such as the abundance,[28] pH sensitivity, [14] and antimicrobial [29] properties. The purpose of this work is to evaluate the use of biopolymers, specifically chitosan, as a base-material for templated hydrogel foams, and the use of these hydrogel foams for water retention purposes.

2. Materials and Methods

2.1 Materials

For the aqueous phase: low molecular weight (50 – 190 kDa) chitosan (75-85% deacetylated, purchased from Sigma-Aldrich), Pluronic F68 (provided by BASF), DI water, and

glacial acetic acid (>99% purchased from Sigma-Aldrich) were used. For the crosslinking mechanism glutaraldehyde (purchased from Sigma-Aldrich, Grade II, 25% in water) was used. For the disperse phase of the emulsion-templating method cyclohexane (purchased from Parmco-Aaper, 99.8%) was used. The compositions of the aqueous solution and sample compositions are in the proceeding tables. The naming of the samples includes the templating method (Foam = F, Froth = Fr, and HIPE = H), disperse phase vol.% (G/W), chitosan and acetic acid wt.% (C:A), and the glutaraldehyde concentration (Glu). For example, the sample, F75_(2:2)_10, is Foam-templated, , 75 vol.% disperse phase, 2 wt.% chitosan, 2 wt.% acetic acid and 10wt.% glutaraldehyde with respect to chitosan's mass. The compositions of the aqueous solution and sample compositions are in the proceeding tables.

Table 1. Aqueous phase composition of chitosan foams with respect to aqueous solution.

	Foam Wt.%	Froth Wt.%	HIPE Wt.%
Chitosan	1-2%	2%	2%
Acetic acid	1-2%	2%	2%
Water	86 – 88%	86%	86%
Pluronic F68	10%	10%	10%
Glutaraldehyde	0.05% - 0.10%	0.10%	0.10%

Table 2. Sample composition of chitosan foams made with three different templating methods: Foam-templating (F), HIPE-templating (H), Froth-templating (Fr). The frothing sample's ϕ_{disp} is an approximation from the change in foam volume size.

Sample	ϕ_{disp} (vol.%)	Chitosan (wt.%)	Acetic acid (wt.%)	Glutaraldehyde (wt.%)
F75_(2:2)_10	75%	2%	2%	0.10%
H75_(2:2)_10	75%	2%	2%	0.10%
Fr_(2:2)_10	~75%	2%	2%	0.10%

2.2 Rheology

The crosslinking of a 1 wt.% chitosan solution was performed in a TA Instrument Discovery HR-3 rheometer while measuring the viscoelastic moduli using oscillatory shear in the linear viscoelastic regime with fixed frequency (10 rad/s) and strain (5%) under time sweep condition at 25 ºC. The glutaraldehyde was added, in excess, at a 5% and 10% (w/w) ratio with respect to the chitosan, equivalent to 50, 100 µl to 1 ml of 1 wt.% chitosan aqueous solution.

2.3 Foam Templating

The aqueous phase components (water, chitosan, acetic acid and Pluronic F68) were mixed using an IKA RW 20 digital overhead mixer at 200 RPM (lowest mixing speed to prevent bubbling of the aqueous phase). Syringes were connected by a three-way locking stopcock that would allow fluid to pass through 2 syringes at once. Each syringe contained a different component: aqueous phase, gas phase and crosslinking agent. Two syringes were connected at a 90º angle and pumped back-and-forth repeatedly for 30 seconds at a rate of 3 pumps/second (Figure 1A). The syringe containing glutaraldehyde was then connected and mixed back-and-

forth 3 times to ensure mixing (Figure 1B). The stopcock was then closed to isolate the foam into one syringe and allowed to crosslink at room temperature. Once crosslinked the foam was removed from the syringe and dried under fume hood.

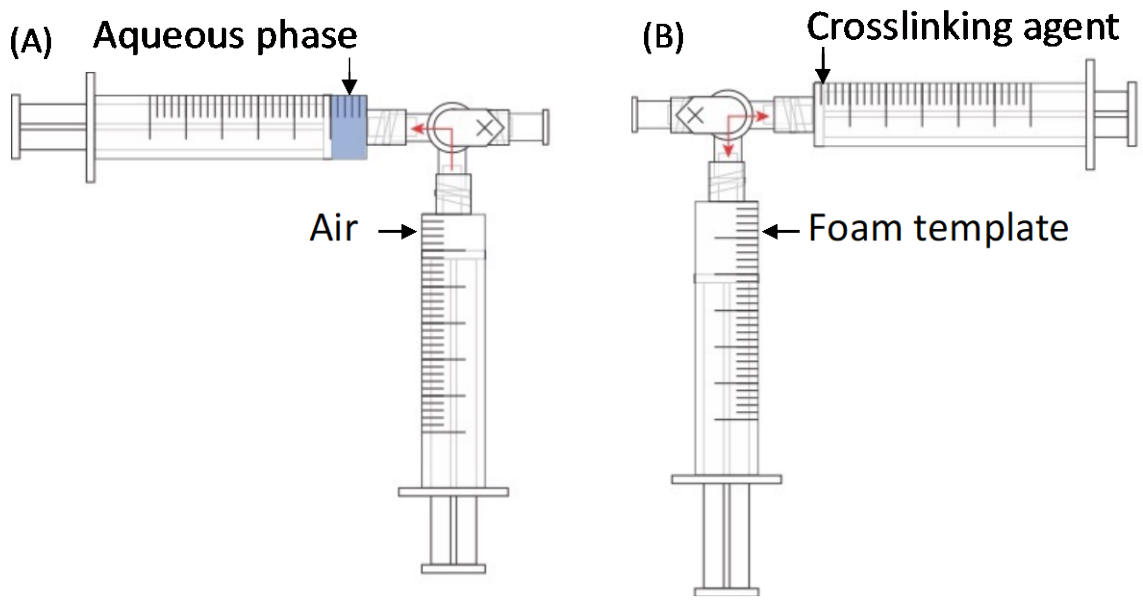

Figure 1. Schematic of the 3-syringe foam-templated mixing method, (A) foaming setup (B) crosslinking set up.

2.4 Frothing Method

The aqueous phase was frothed using an IKA RW 20 digital overhead mixer at 2000 RPM for 10 minutes. The glutaraldehyde was then injected directly into the foam and mixed for 30 more seconds to ensure good mixing. The beaker was then covered and allowed to crosslink at room temperature. Once crosslinked the foam was removed from the syringe and dried under fume hood.

2.5 Emulsion Templating

High internal phase emulsions were made through the conventionally used method by means of mechanical mixing (Figure 2).[30] The aqueous phase was mixed first at 200 RPM using an IKA RW 20 digital overhead mixer until homogenous. The disperse phase, cyclohexane, was added by an automated syringe pump (KD Scientific 120 Push/Pull Syringe Pump) while mixing at 500 RPM. To ensure the correct volume of cyclohexane was added, the emulsion was weighed before and after the dispersion accounting for evaporated cyclohexane during addition and emulsification. The crosslinking, glutaraldehyde, was added at a 10 wt.% equivalent to the chitosan mass and mixed with a micro spatula for 30 seconds to ensure good distribution. Once crosslinked the foam was removed from the syringe and dried under fume hood.

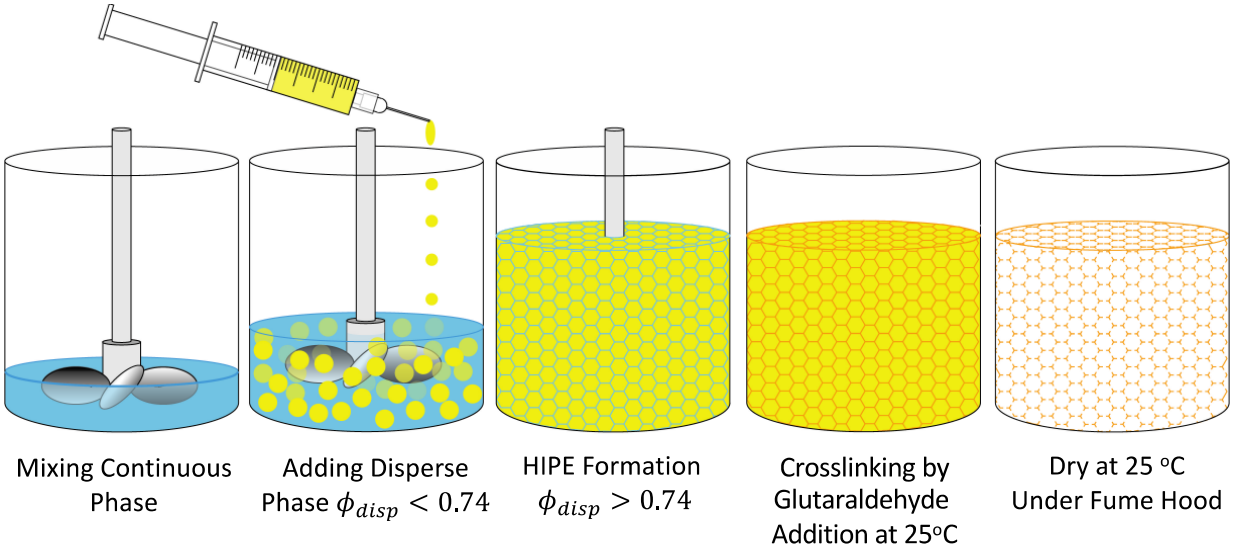

Figure 2. Schematic of chitosan polyHIPE formation

2.6 Porosity

The porosity was measured by weighing the initial mass of a sample and then immersing it in melted soy wax to create a thin hydrophobic barrier preventing water sorption. The sealed sample was then immersed in a volumetric flask to measure the displacement volume using image analysis through AM Scope software. The density ratio of the foam to the non-porous bulk material is used to calculate the porosity of the samples.

2.7 Scanning Electron Microscope

Polymerized foam samples were frozen in liquid nitrogen and crushed. The surfaces of broken pieces were then sputter coated using a gold filament in a Denton Desk IV Sputter Coater and analyzed with a Hitachi S-3400N Type II scanning electron microscope (SEM). The images were analyzed using AM Scope software to measure void and window diameters (N = 300 per image).

2.8 Water Uptake

The samples were placed in plastic vials followed by an excess addition of DI water. At different time intervals, the water was removed by syringe, the sample was weighed. Fresh DI water was added to continue the experiment at incremental times.

3. Results and Discussion

3.1 Rheology

Time sweep tests of 1wt.% chitosan solutions showed chitosan was a promising candidate for foam-templating methods. Both 5 and 10% (w/w, with respect to chitosan) glutaraldehyde additions showed immediate crosslinking within minutes of application (Figure 5-2). There was also a trend of increased moduli when the crosslinking agent was increased in volume (50 to 100 µl). The storage modulus (G') surpasses the loss modulus (G") indicating a transition from a liquid state to solid due to the crosslinking reaction. This was apparent before the time sweep initiates indicating the crosslinking occurs during the mixing of glutaraldehyde. The fast crosslinking was beneficial for the foam-templating process due to the rapid coalescence of the foam.

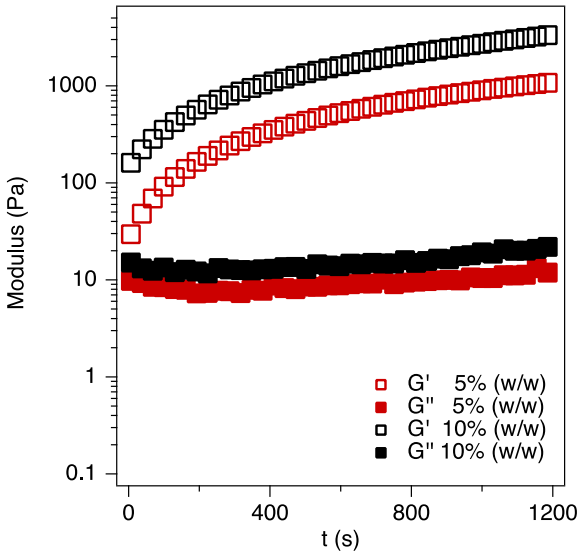

Figure 3. Time sweep of 1wt.% chitosan solution crosslinked with 5% and 10% (w/w) glutaraldehyde with respect to chitosan at 25 ºC. The glutaraldehyde was injected and mixed in with 1 ml of the chitosan solution then placed on the rheometer stage for testing.

3.2 Templated Chitosan Foam Synthesis

During the addition of glutaraldehyde, the HIPE started to change color within minutes of addition indicating crosslinking (from a light yellow to a darker brown color). The resulting emulsion-templated foam resulted in sponge-like material that could easily fracture under small shear forces. In foam templating, after adding the glutaraldehyde, the foam produced heat and noticeably changed in color within several minutes. The resulting foam-templated material resulted in a soft sponge-like material similar to polyurethane foam. The increase in glutaraldehyde concentration, 5 to 10% (w/w) ratio, was noticeably different in material strength. Once the foams were dried, they slightly reduced in volume and became increasingly tough and brittle. This was due to the extremely high concentration of water in the aqueous phase (>80%). In other words, if the aqueous phase is crosslinked under the same conditions (without porosity) and is dried, the bulk material reduces volume enough to become a thin film. This was further proven by measuring the density of the resulting foams. The porosity of samples between the three templating methods were above 90% (Table 3) due to the low amount of base material (chitosan) and high initial water content. The low density of the foams indicates a highly porous structure highly beneficial to porous polymer applications.

Table 3. Density and porosity of chitosan samples with C:A ratio of (2:2), G/W ratio of 0.75 and 10% glutaraldehyde crosslinking.

	PolyHIPE	Froth	Foam	Bulk
Mass (g)	0.008	0.014	0.012	0.048
Volume (ml)	0.200	0.200	0.200	0.050
Density (g/ml)	0.040	0.070	0.060	0.960
Porosity	96%	93%	94%	0%

3.3 Templated Foam Morphology

The resulting morphology of the templated foams observed from the scanning electron microscope was a very porous and interconnected network. The interconnectivity (windows) was primarily dependent on the method of templating and secondly dependent on the sample composition (explored further with varying foam-templating sample compositions). The frothing method provided slightly larger void size in comparison to the syringe method and noticeably larger void walls (Figure 3A). The frothing also showed some window formation between voids but was not widely prevalent. This was likely due to a limitation of bubble breakup using the frothing method.

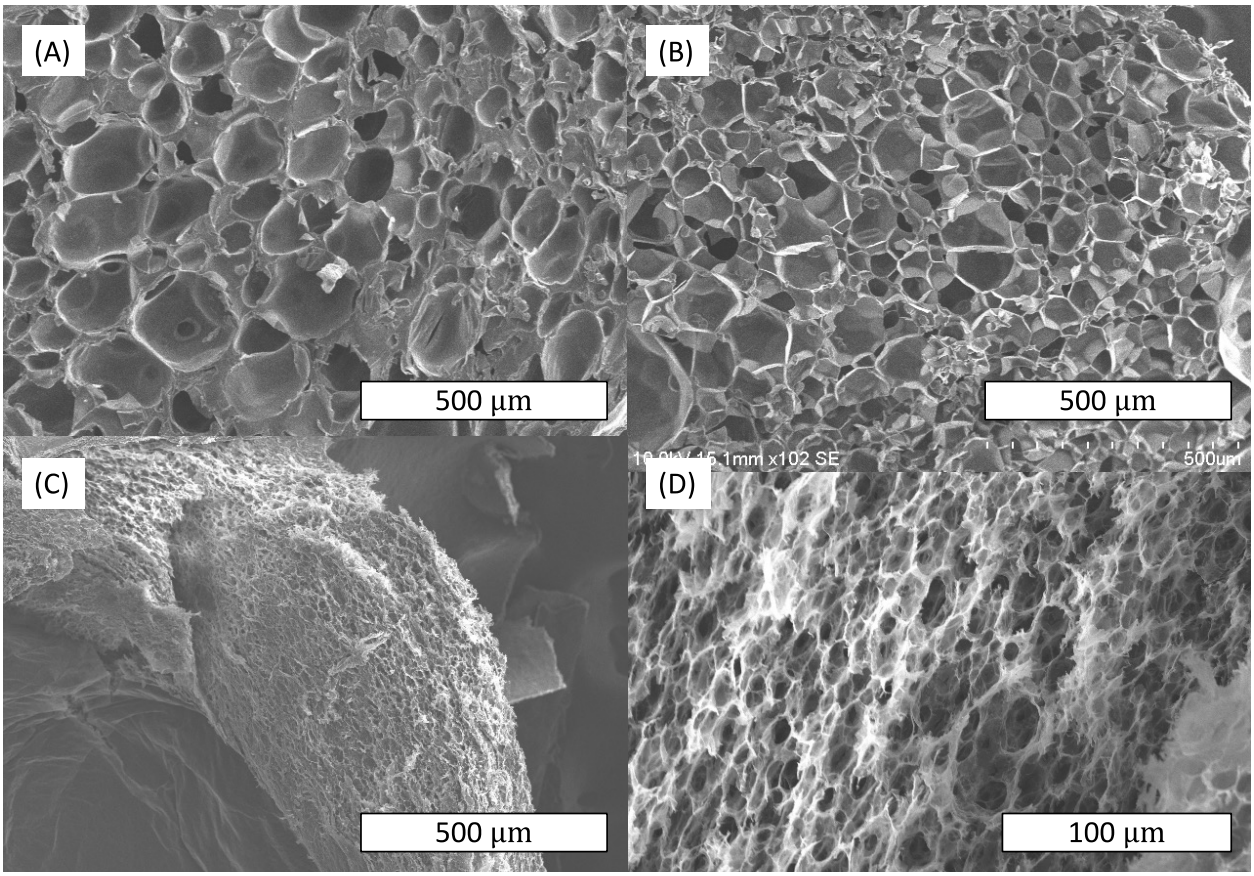

Figure 4. Scanning electron microscope images of chitosan foams varying by templating method: (A) Foam-templated by frothing or froth templated, (B) Foam-templated by gas mixing through pumping back and forth by syringes, and (C & D) HIPE-templated.

The foam-templated method using interconnected syringes shows a smaller void size and more window formation than frothing method (Figure 5-3B). The walls of the voids are noticeably thinner than the frothing method, and thin walls that would likely form windows (similar to SEM images from Chapter 3) are also common. The deformation force caused by extensional flow between the syringes was more effective in mixing and bubble breakup than the shear stress in overhead mixer used for the frothing method. In addition, the closed system of the syringe also likely played a role in the stability of the foam (during crosslinking), preventing the bubbles from coalescing and forming larger bubbles.

The HIPE-templating method provided a significantly lower void size than the gas-templated systems (Figures 5-3C and D). This was likely due to the higher stability as a result of lower interfacial tension in emulsion systems as discussed in Chapter 2. There was also a higher prevalence of windows likely due to the closer packing of droplets and less competition between the interfacial film and depletion attraction during the crosslinking. While the focus on this chapter is the foam-templating method, these other templating systems showed a range of morphology that expands the applicability of the porous chitosan-based hydrogels.

The compositions of foam-templated samples were varied to understand the determinant factors in the resulting foam morphology. The goal is to determine these factors so the foam-templating method can be effectively scaled up for producing stable foam templates that result in the desired foam morphology. The results are broken into two figures based on crosslinking (w/w) ratio at 5% (Figure 5-4) and 10% (Figure 5-5) with respect to chitosan wt.%.

The most noticeable difference in the SEM between both figures was the difference in morphology as the G/W ratio increases. For the 1 wt.% chitosan samples, with 5% Glu, the void size was less defined and gets larger. This was likely due to higher instability from the higher gas dispersion. For 10% Glu, the foam structure was not as disrupted since the crosslinking rate was faster, thus, preventing foam coalescence. However, the void sizes are getting larger due to the higher instability with the increase in G/W.

For the 2 wt.% chitosan samples, the resulting foams had lower void size as the G/W ratio increased (in comparison to 1 wt.% chitosan samples) and had better void definition with lower crosslinking (5% glutaraldehyde). However, there was still apparent instability at higher G/W ratios for the 2 wt.% chitosan. The reason for the 2 wt.% chitosan's behavior was likely due to higher viscosity as a result of higher chitosan concentration. Higher viscosity can lead to higher

foam stability by reducing drainage rate of the foam that in turn preserves the film between bubbles. [31]

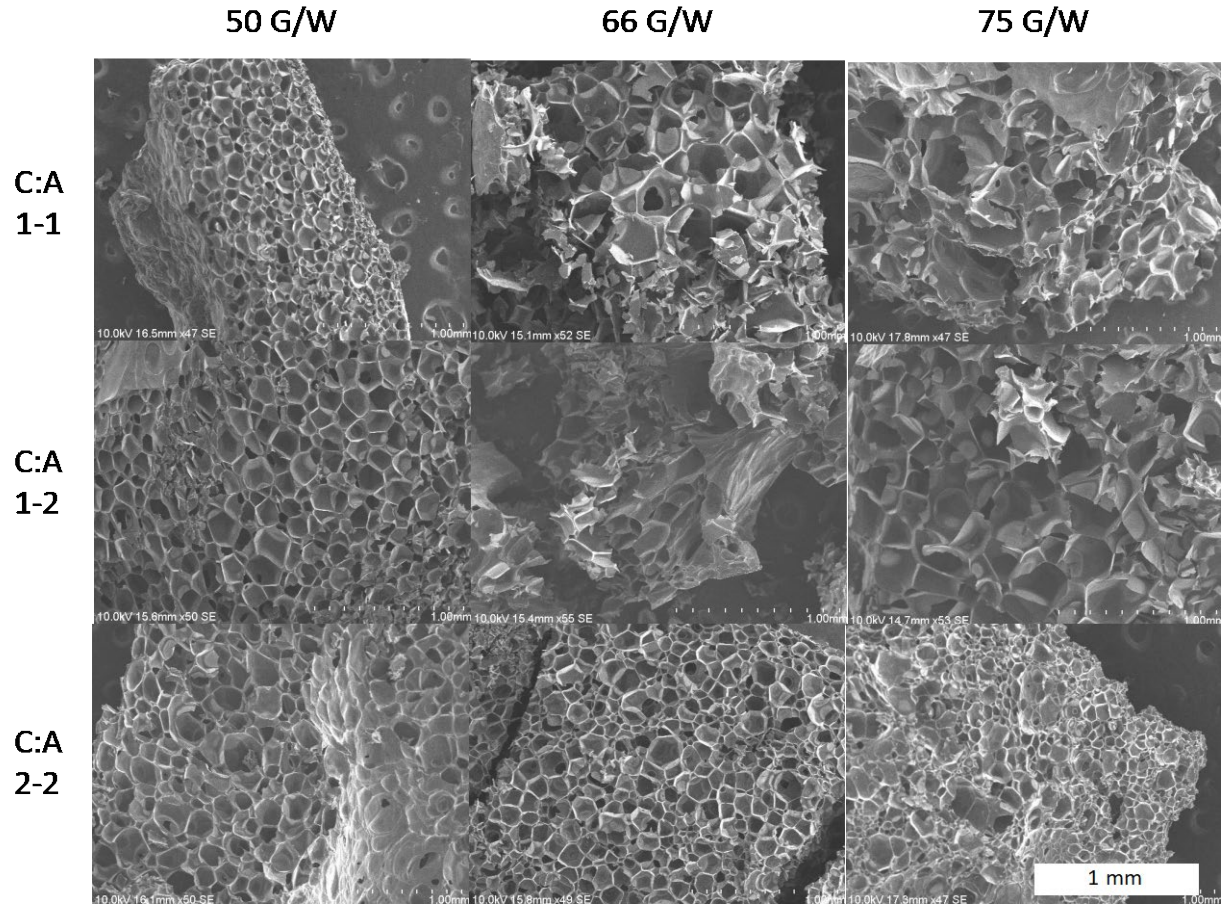

Figure 5. SEM of foam-templated chitosan with 5% (w/w) glutaraldehyde crosslinking varying in chitosan-to-acetic acid (w/w) ratio (C:A) and gas-to-water phase (v/v) ratio (G/W).

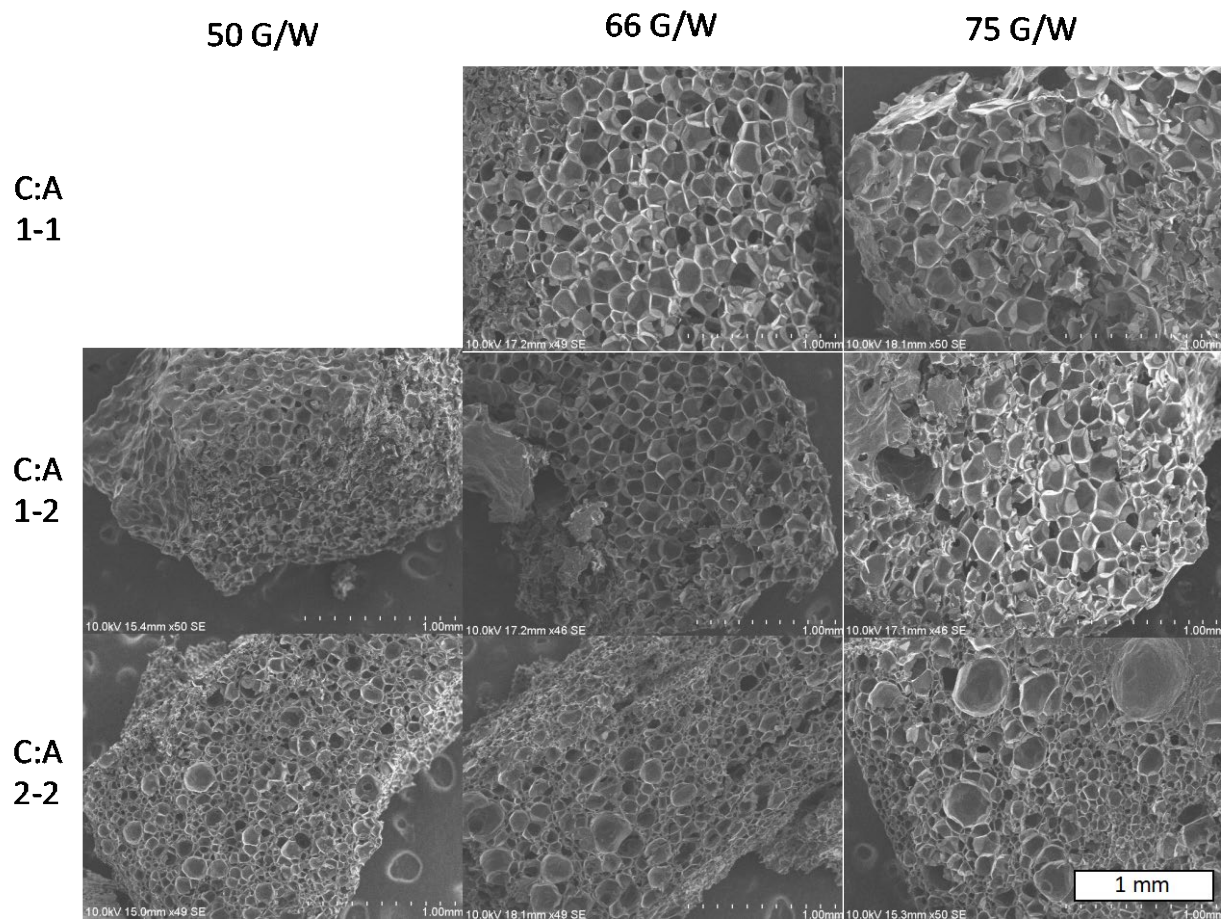

Figure 6. SEM of foam-templated chitosan with 10% (w/w) glutaraldehyde crosslinking varying in chitosan-to-acetic acid (w/w) ratio (C:A) and gas-to-water phase (v/v) ratio (G/W).

Table 4. Data of scanning electron microscope analysis of foam-templated (F), froth-templated (Fr) and HIPE-templated (H) chitosan foams. The samples are broken into columns by their approximate disperse phase volume fraction (ϕ_{disp} = 0.50, 0.66 and 0.75). The samples separated in rows by chitosan-to-acetic acid (w/w) concentration (C:A = 1:1, 1:2 and 2:2), and by glutaraldehyde (w/w) concentration (Glu = 5 or 10). Average void diameters (D_v) ± standard error.

$\phi_{disp} = 0.50$	D_v (μm)	$\phi_{disp} = 0.66$	D_v (μm)	$\phi_{disp} = 0.75$	D_v (μm)
F50_(1:1)_5	89.1 ± 5.1	F66_(1:1)_5	106.5 ± 5.1	F75_(1:1)_5	137.4 ± 5.1
F50_(1:2)_5	92.8 ± 1.5	F66_(1:2)_5	129.2 ± 6.5	F75_(1:2)_5	129.2 ± 6.1
F50_(2:2)_5	164.3 ± 5.8	F66_(2:2)_5	70.0 ± 2.3	F75_(2:2)_5	51.1 ± 2.1
F50_(1:1)_10	232.0 ± 7.8	F66_(1:1)_10	116.3 ± 6.2	F75_(1:1)_10	162.9 ± 4.6
F50_(1:2)_10	161.9 ± 6.6	F66_(1:2)_10	81.2 ± 3.6	F75_(1:2)_10	151.3 ± 4.8
F50_(2:2)_10	111.0 ± 2.2	F66_(2:2)_10	61.9 ± 1.9	F75_(2:2)_10	75.0 ± 3.1
				H75_(2:2)_10	16.3 ± 0.7
				Fr75_(2:2)_10	99.1 ± 3.7

3.4 Water Uptake Results

The water uptake tests show templated chitosan foams have rapid water uptake capabilities (Figure 6). The selected samples used for water uptake are chosen to compare the different parameters of the synthesized foam-templated samples: G/W ratio, C:A ratio and Glu concentration. The water uptake has a slight increase as the C:A ratio increases to 2:2 likely due to a more defined porous morphology resulting from a more viscous solution with higher foam stability. This was most noticeable in the 50% G/W set of samples. The increase in acetic acid in the (1:2) set of samples did not significantly influence the resulting water uptake samples, except for the 75 G/W ratio. For this case, the increase in chitosan hydrolysis may have helped the

bubble breakup mechanism, and thus, the resulting foam structure. Comparing the water uptake among samples with different G/W ratios did not show a typical tend (i.e., porosity dominant or crosslinking dominant). For a majority of samples, the 66 G/W ratio sample had a consistently higher water uptake (excluding F66_(2:2)_10). The likely reason for this was the higher stability of 66 G/W in comparison to 75 G/W, and thinner films between bubbles in comparison to 50 G/W. This results in a foam with smaller void size and higher window propagation. When comparing the templating methods, the HIPE-templated chitosan foam showed to have the highest initial water uptake due to the small void size of the polyHIPE as well as the high interconnectivity. Whereas the froth-templated chitosan had the lowest water uptake for having the largest voids and lowest interconnectivity. While the initial water uptake was improved with the improved morphology, the maximum water uptake appeared to be limited by the porosity of the foam considering how the HIPE-templated and foam-templated porous hydrogels differ in morphology but have nearly the same porosity.

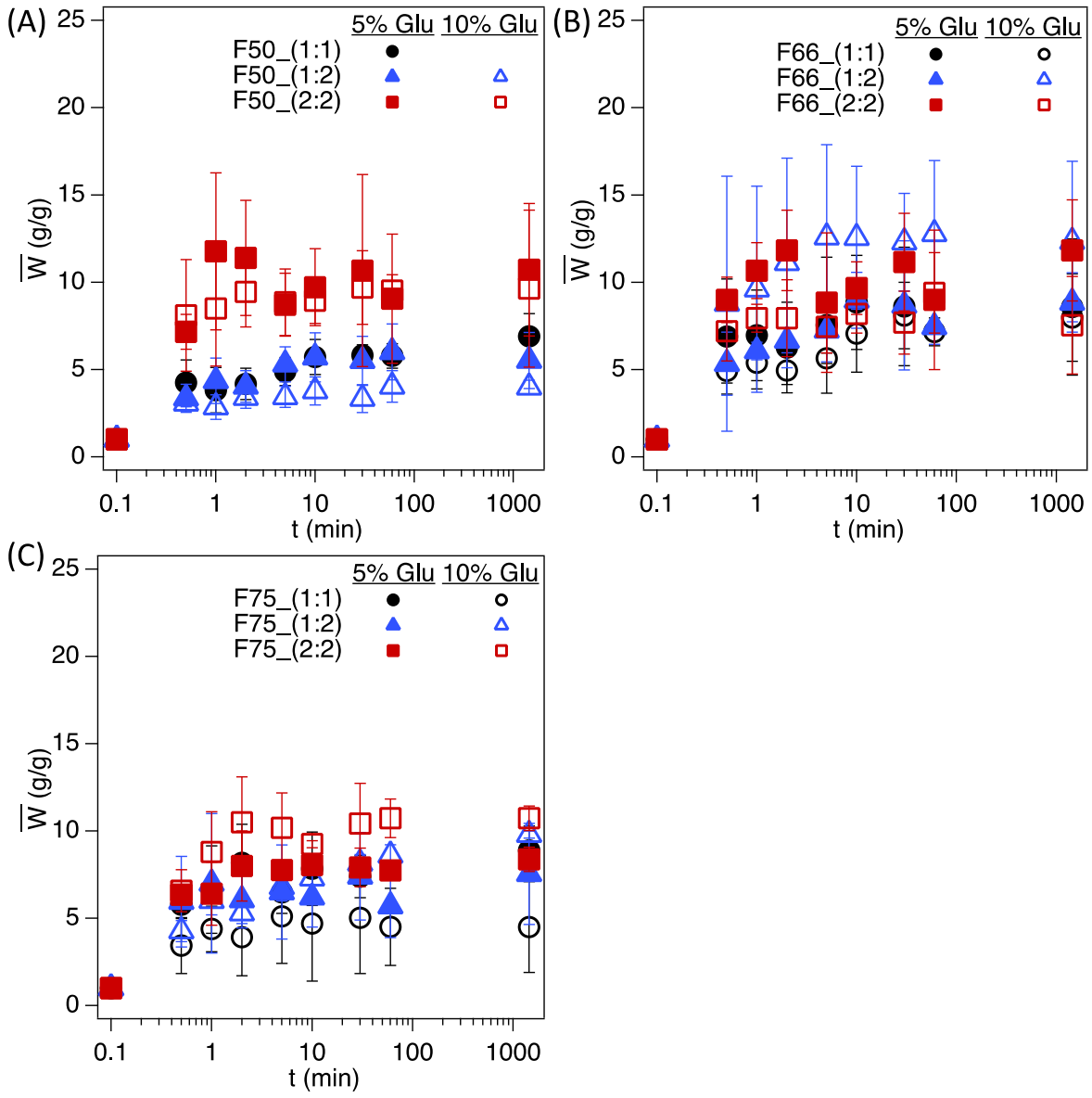

Figure 7. (A, B and C) Water uptake of foam-templated chitosan hydrogels varying in C:A ratio and glutaraldehyde concentration. (D) Water uptake of chitosan varying in templating method: foam (F), froth (Fr) and HIPE (H).

4. Conclusions

There is an appeal to a completely biodegradable porous hydrogel for various applications. Due to foam's high capillary action and increased surface area of these foams they

can improve many applications that utilize polysaccharide-based hydrogels. Foam-templating of hydrogels is a difficult method to implement due to high foam instability. This requires rapid curing times to solidify the foam before the bubbles become too large due to coalescence. From rheological studies the crosslinking mechanism between chitosan and glutaraldehyde is a rapid process that can be used successfully for foam-templating, froth-templating, and emulsion-templating methods.

From this work we show a successfully generated chitosan-based foam, with the forementioned methods, with rapid water uptake and high water sorption capabilities. By comparing the SEM images and water uptake tests, there is a clear relationship between the hydrogel morphology and its water sorption properties. Thus, the main parameters to change the material properties are the viscosity of the aqueous solution by chitosan concentration and the rate of crosslinking by glutaraldehyde addition. Due to the applicability of these templating methods, other materials can be utilized that possess rapid curing properties and can be tuned through sample composition. Biopolymers are good applicants for these templating methods considering biopolymer solutions are typically viscous and contain similar crosslinking functional groups which can lead to good foam stability and rapid crosslinking, respectively. While we utilized chitosan for this work there are many other bio-based polymers that can be utilized using the FT method due to their rapid crosslinking. One example that will be studied further is sodium alginate, a polysaccharide that can be ionically crosslinked instantaneously by calcium chloride solution and covalently crosslinked by a crosslinking agent (i.e., epichlorohydrin). The main takeaway from this work is the potentially economically viable foam-templating method that can be applied to various combinations of bio-based polymers.

References:

(1) Boretti, A.; Rosa, L. Reassessing the Projections of the World Water Development Report. *npj Clean Water* **2019**, *2*, 1–6.

(2) Irrigation and Water Use https://www.ers.usda.gov/topics/farm-practices-management/irrigation-water-use/ (accessed May 1, 2018).

(3) Longworth, J. W.; Valdez, J. M.; Magnuson, M. L.; Richard, K. *New Mexico Water Use by Categories 2010*; Santa Fe, NM, 2013.

(4) Kühn-institut, J. Biological Degradability of Syntetic Superabsorbent Soil Conditioners Aus Dem Institut Für Pflanzenernährung Und Bodenkunde Martin Wolter Frantisek Zadrazil Joachim Haselbach Carsten in Der Wiesche Sigrid Hey Ewald Schnug Biologische Abbaubarkeit Syntheti. **2016**, No. January 2002.

(5) Cameron, M. D.; Post, Z. D.; Stahl, J. D.; Haselbach, J.; Aust, S. D. Cellobiose Dehydrogenase-Dependent Biodegradation of Polyacrylate Polymers by Phanerochaete Chrysosporium. *Environ. Sci. Pollut. Res.* **2000**, *7*, 130–134.

(6) Wilske, B.; Bai, M.; Lindenstruth, B.; Bach, M.; Rezaie, Z.; Frede, H. G.; Breuer, L. Biodegradability of a Polyacrylate Superabsorbent in Agricultural Soil. *Environ. Sci. Pollut. Res.* **2014**, *21*, 9453–9460.

(7) Sutradhar, S. C.; Khan, M. M. R.; Rahman, M. M.; Dafadar, N. C. The Synthesis of Superabsorbent Polymers from a Carboxymethylcellulose/Acrylic Acid Blend Using Gamma Radiation and Its Application in Agriculture. *J. Phys. Sci.* **2015**, *26*, 23–39.

(8) Zhou, S. Injectable Polysaccharide Scaffolds for Soft Tissue Engineering Prepared By O / W High Internal Phase, Imperial College London, 2010.

(9) Pourjavadi, A.; Hossein, G.; Mojahedi, F. Swelling Properties of CMC-g-Poly (AAm-Co-AMPS) Superabsorbent Hydrogel. *J. Appl. Polym. Sci.* **2009**, *113*, 3442–3449.

(10) Guan, Y.; Cui, H.; Ma, W.; Zheng, Y.; Tian, Y.; Hu, J. An Enhanced Drought-Tolerant Method Using SA-Loaded PAMPS Polymer Materials Applied on Tobacco Pelleted Seeds. *Sci. World J.* **2014**, *2014*.

(11) Chandrika, K. P.; Singh, A.; Rathore, A.; Kumar, A. Novel Cross Linked Guar Gum-g-Poly(Acrylate) Porous Superabsorbent Hydrogels: Characterization and Swelling Behaviour in Different Environments. *Carbohydr. Polym.* **2016**, *149*, 175–185.

(12) A., A. E. H. Characterization and Possible Agricultural Application of Polyacrylamide/Sodium Alginate Crosslinked Hydrogels Prepared by Ionizing Radiation. *J. Appl. Polym. Sci. 101*, 3572–3580.

(13) Cascone, S.; Lamberti, G. Hydrogel-Based Commercial Products for Biomedical Applications: A Review. *Int. J. Pharm.* **2020**, *573*, 118803.

(14) Shen, X.; Shamshina, J. L.; Berton, P.; Gurau, G.; Rogers, R. D. Hydrogels Based on Cellulose and Chitin: Fabrication, Properties, and Applications. *Green Chem.* **2016**, *18*, 53–75.

(15) Silverstein, M. S. Emulsion-Templated Porous Polymers: A Retrospective Perspective. *Polym. (United Kingdom)* **2014**, *55*, 304–320.

(16) Zhang, T.; Sanguramath, R. A.; Israel, S.; Silverstein, M. S. Emulsion Templating: Porous Polymers and Beyond. *Macromolecules* **2019**, *52*, 5445–5479.

(17) Choudhury, S.; Connolly, D.; White, B. Supermacroporous PolyHIPE and Cryogel Monolithic Materials as Stationary Phases in Separation Science: A Review. *Anal. Methods* **2015**, *7*, 6967–6982.

(18) Guarino, V.; Caputo, T.; Altobelli, R.; Ambrosio, L. Degradation Properties and Metabolic Activity of Alginate and Chitosan Polyelectrolytes for Drug Delivery and Tissue Engineering Applications. *AIMS Mater. Sci.* **2015**, *2*, 497–502.

(19) Baniasadi, H.; Mashayekhan, S.; Fadaoddini, S.; Haghirsharifzamini, Y. Design, Fabrication and Characterization of Oxidized Alginate-Gelatin Hydrogels for Muscle Tissue Engineering Applications. *J. Biomater. Appl.* **2016**, *31*, 152–161.

(20) Yang, C. H.; Wang, M. X.; Haider, H.; Yang, J. H.; Sun, J. Y.; Chen, Y. M.; Zhou, J.; Suo, Z. Strengthening Alginate/Polyacrylamide Hydrogels Using Various Multivalent Cations. *ACS Appl. Mater. Interfaces* **2013**, *5*, 10418–10422.

(21) Jeon, O.; Shin, J. Y.; Marks, R.; Hopkins, M.; Kim, T. H.; Park, H. H.; Alsberg, E. Highly Elastic and Tough Interpenetrating Polymer Network-Structured Hybrid Hydrogels for Cyclic Mechanical Loading-Enhanced Tissue Engineering. *Chem. Mater.* **2017**, *29*, 8425–8432.

(22) Zowada, R.; Foudazi, R. Polyfoam: Foam-Templated Microcellular Polymers. *Langmuir* **2020**, *36*, 7868–7878.

(23) Maity, S.; Sa, B. Development and Evaluation of Ca+ 2 Ion Cross-Linked Carboxymethyl Xanthan Gum Tablet Prepared by Wet Granulation Technique. *AAPS PharmSciTech* **2014**, *15*, 920–927.

(24) Hongbo, T.; Yanping, L.; Min, S.; Xiguang, W. Preparation and Property of Crosslinking Guar Gum. *Polym. J.* **2012**, *44*, 211–216.

(25) Pavoni, J. M. F.; dos Santos, N. Z.; May, I. C.; Pollo, L. D.; Tessaro, I. C. Impact of Acid Type and Glutaraldehyde Crosslinking in the Physicochemical and Mechanical Properties and Biodegradability of Chitosan Films. *Polym. Bull.* **2021**, *78*, 981–1000.

(26) Badawy, M. E. I.; Taktak, N. E. M.; Awad, O. M.; Elfiki, S. A.; El-Ela, N. E. A. Preparation and Characterization of Biopolymers Chitosan/Alginate/Gelatin Gel Spheres Crosslinked by Glutaraldehyde. *J. Macromol. Sci. Part B Phys.* **2017**, *56*, 359–372.

(27) Liu, Y.; Cai, Z.; Sheng, L.; Ma, M.; Xu, Q.; Jin, Y. Structure-Property of Crosslinked Chitosan/Silica Composite Films Modified by Genipin and Glutaraldehyde under Alkaline Conditions. *Carbohydr. Polym.* **2019**, *215*, 348–357.

(28) Sharp, R. A Review of the Applications of Chitin and Its Derivatives in Agriculture to Modify Plant-Microbial Interactions and Improve Crop Yields. *Agronomy* **2013**, *3*, 757–793.

(29) Kumirska, J.; Czerwicka, M.; Kaczyński, Z.; Bychowska, A.; Brzozowski, K.; Thöming, J.; Stepnowski, P. Application of Spectroscopic Methods for Structural Analysis of Chitin and Chitosan. *Mar. Drugs* **2010**, *8*, 1567–1636.

(30) Zowada, R.; Foudazi, R. Porous Hydrogels Embedded with Hydrated Ferric Oxide Nanoparticles for Arsenate Removal. *ACS Appl. Polym. Mater.* **2019**, *1*, 1006–1014.

(31) Jiang, Q.; Bismarck, A. A Perspective: Is Viscosity the Key to Open the next Door for Foam Templating? *React. Funct. Polym.* **2021**, *162*, 104877.